An Impedance-Based Model for the Evaluation of IM3 in Nonlinear Amplifiers Showing Memory Effects

María J. Madero-Ayora, Javier Reina-Tosina, Carlos Crespo-Cadenas
Dept. de Teoría de la Señal y Comunicaciones
Escuela Superior de Ingenieros, Universidad de Sevilla
Camino de los Descubrimientos, s/n.; 41092 – Seville, Spain
Phone: +34 95 4487290; Fax: +34 95 4487341; E-mail: mjmadero@us.es

Abstract

A simple model that captures nonlinear memory effects in wideband amplifiers is presented in this work. The model defines an equivalent hypothetical load impedance that explains asymmetries, in magnitude and phase, in two-tone IM products, showing good correspondence with measurements. It helps to understand the IMD dependence on modulation bandwidth.

Index Terms

Two-tone measurements, nonlinear distortion in amplifiers, intermodulation products, memory effects, impedance-based model.

I. INTRODUCTION

The search for higher efficiency amplifiers has propelled the interest of researchers in nonlinear effects emerged when circuits are excited with RF communication signals with a level near their compression point. The use of this type of signals makes necessary new design parameters such as spectral regrowth and adjacent-channel power, and enforces a refinement of device modeling techniques, simulation approaches, and experimental characterization. Nevertheless, two-tone intermodulation distortion (IMD) measurements still play an outstanding role among nonlinear experimental characterization methods. Starting from a two-tone test it is possible to predict the behavior of distortion components for more complex modulations exhibiting wide bandwidths, such as those employed in modern communication signals.

Regarding this aspect, a restrictive issue in the design of wideband amplifiers with low distortion and high efficiency is the IMD dependent on modulation bandwidth. Traditionally, technical datasheets of commercial RF and microwave circuits show the nonlinear performance using an arbitrary modulation bandwidth. However, IMD levels can experience significant variations when excitations with different bandwidths are tested. This phenomenon is the result of complex interactions inside the active devices and with the rest of the circuit, which are known as memory effects and make distortion strongly dependent on the characteristics of the modulation signal. These effects represent a challenge to the success of linearization methods, especially for those trying to accomplish IMD reduction by applying the excitation signal corrupted by a similar distortion with opposite phase, as is the case of digital predistortion.

Memory effects can be defined as shifts in the amplitude and phase of IMD components caused by changes in the modulation frequency [1]. They can be produced by electrical and thermal causes, the latter affecting mainly low modulation frequencies [2]. Traditional modeling methods do not have the capability to estimate the dependence of IMD on bandwidth, but these effects must be taken into account when designing high efficiency amplifiers in order to satisfy the strict requirements demanded over increasingly growing bandwidths. The need for models that allow the prediction of memory effects is thus justified. It is quite common to derive these kinds of models from measurements. A two-tone test signal with varying tone separations can be used for experimental characterization of memory effects, being advisable measurements for both magnitude and phase of the intermodulation (IM) products. In [3], the authors presented a novel

approach for the measurement of two-tone IMD asymmetries. This method was subsequently applied to derive closed-form expressions for magnitude and phase of third- and fifth-order IMD (IM3 and IM5, respectively) of a HEMT transistor [4]. The obtained theoretical expressions showed some discrepancies with the measured variation of IM3 for small tone separations. A simplified model based on finding an equivalent hypothetical load impedance that can explain discrepancies between measurements and circuit-level predictions was proposed in [5] and the results were generalized in [6] for the case of a commercial amplifier exhibiting memory effects, without prior knowledge of the internal structure of the circuit. In this work, we apply them in order to demonstrate the good correspondence with measurements achieved by using a simple impedance-based model.

II. Methodology

The approach explained in the present work consists in finding an equivalent hypothetical load impedance that is responsible for IMD asymmetries and the bandwidth dependent IMD behavior of a microwave amplifier. This equivalent load impedance is extracted from experimental measurements of IM products that are compared with theoretical expressions, in a similar way to the work of Brinkhoff [7]. The main difference between both works is that the theoretical expressions presented here are derived from a Simplified-Newton (SN) approach combined with the Nonlinear Currents (NC) method, while Brinkhoff's expressions are derived from a Volterra series analysis.

A. Elementary HEMT amplifier analysis

Let consider the equivalent two-node circuit model of an elementary HEMT amplifier shown in Fig. 1(a), where only the most significant nonlinearity, i.e. the drain current source, has been considered. We can express the drain current as a double Taylor-series expansion, truncated up to third order terms ($N = 3$) of the gate v_g and drain v_d voltages under the assumption of weakly nonlinear behavior:

$$I[V_G + v_g(t), V_D + v_d(t)] = I_{DC} + g_{10}v_g(t) + g_{01}v_d(t) + i_{NL}[v_g(t), v_d(t)]$$

$$i_{NL}[v_g(t), v_d(t)] = \sum_{k=2}^{N} g_{k0}v_g^k(t) + \sum_{l=2}^{N} g_{0l}v_d^l(t) + \sum_{\substack{k,l=1 \\ k+l<N}} g_{kl}v_g^k(t)v_d^l(t), \qquad (1)$$

where the terms g_{kl} are bias-dependent coefficients. The circuit used in the analysis accounts for any existing extrinsic elements with the load and source impedances, which are frequency-dependent impedances, $Z_L(f)$ and $Z_s(f)$ respectively. A two-tone input signal is considered and expressed in the form $v_s(t) = \Re\{\tilde{v}_s(t)e^{j\omega_c t}\}$, where the complex envelope is $\tilde{v}_s(t) = 2A\cos(\omega_m t)$ with A real. The analysis assumes a narrow-band RF input signal, i.e. the tone frequency spacing Δf does not exceed a certain value, and is based on the application of the NC method, where a SN approach [4] has been taken into account in order to obtain the nonlinear currents expressions. The following closed-form expressions are obtained for the drain voltage components at tone frequencies and IM3:

$$\begin{aligned} V_{h,l} &= H_1 A + \left[\tfrac{9}{4}\gamma_3 + \gamma'_{20}\bar{Z}_L(\pm\Delta f)\right] A^3 \\ V_{3h,3l} &= \left[\tfrac{3}{4}\gamma_3 + \gamma'_{20}\bar{Z}_L(\pm\Delta f)\right] A^3, \end{aligned} \tag{2}$$

where $\bar{Z}_L(\pm\Delta f)$ represents the load impedance seen by the drain source at baseband frequencies, and the γ-functions are expressed in terms of the drain and gate linear transfer functions, and of the impedance relating the components of the nonlinear currents with node voltages at the fundamental and second-harmonic frequency zones. Therefore, for a given carrier frequency, the values γ'_{20} and γ_3 are bias-dependent constants.

It should be remarked that none of the terms in (2) depends on frequency except for $\bar{Z}_L(\pm\Delta f)$. Furthermore, this approach separates the load impedance influence from the rest of electrical parameters and shows its predominant role in the generation of memory effects. Analogous results are obtained in [7] using a Volterra Series approach, limited to third-order terms. It is worth noticing that the only difference between the expression for the lower IM3 ($\mathrm{IM_{3L}}$), expressed by the component V_{3l}, and the upper IM3 ($\mathrm{IM_{3H}}$), expressed by the component V_{3h}, is the presence of $\bar{Z}_L(\Delta f)$ in the latter and $\bar{Z}_L(-\Delta f) = \bar{Z}_L^*(\Delta f)$ in the former. If the γ_3-term has a negligible imaginary part, then the magnitudes of $\mathrm{IM_{3L}}$ and $\mathrm{IM_{3H}}$ will be nearly the same and no asymmetry will be detected if only power measurements of the IM products have been achieved. This fact emphasizes the importance of phase measurements in two-tone tests.

Since the experimental setup used for IM3 characterization in this work supplies phase measurements relative to the tones, the expressions for the voltages of $\mathrm{IM_{3L}}$ and $\mathrm{IM_{3H}}$ relative

to the lower and upper tones will be considered:

$$F_{3h} = \frac{\left[\frac{3}{4}\gamma_3 + \gamma'_{20}\bar{Z}_L(\Delta f)\right] A^2}{H_1 + \left[\frac{9}{4}\gamma_3 + \gamma'_{20}\bar{Z}_L(\Delta f)\right] A^2}$$
$$F_{3l} = \frac{\left[\frac{3}{4}\gamma_3 + \gamma'_{20}\bar{Z}^*_L(\Delta f)\right] A^2}{H_1 + \left[\frac{9}{4}\gamma_3 + \gamma'_{20}\bar{Z}^*_L(\Delta f)\right] A^2}. \tag{3}$$

Following (3), a prediction of the variation with frequency shown by IM3 can be determined by using $\bar{Z}_L(\Delta f)$, which must include all the intrinsic and extrinsic elements in the circuit connected to the drain node. However, if the amplifier shows low frequency dispersive effects (including dispersion due to self-heating, impact ionization, or trapping effects), circuit-level simulations accomplished using the SN approach will not fit measurements for the lower tone separations. The basic idea under this approach is that the extraction of an appropriate hypothetical load impedance, using measurements of both magnitude and phase, must be able to provide a good agrement with two-tone IM measurements, regardless the memory effects that cause the asymmetry are of electrical or thermal origin. Furthermore, a part of the load impedance seen by the drain node will be known, that is, the elements of the intrinsic model of the HEMT connected to the drain node, the impedance of the bias network, and the impedance placed at the output of the amplifier. Once the values for the equivalent load impedance that fit measurements have been obtained, all known elements can be de-embedded and the remaining term will be a hypothetical electrical impedance Z_h, which accounts for electrothermal effects and is not included in the device model. In Section III, a circuit model for the impedance Z_h will be obtained and discussed for a certain group of measurements.

B. Impedance-based model for commercial amplifiers

The theoretical results obtained for a HEMT device in the previous section can be generalized to more complex circuits provided that they exhibit a moderate gain, and high reverse isolation at low frequencies. These assumptions are common in amplifiers, for which we propose the following extension:

$$V_{3h,3l} = \sum_{\substack{n=3 \\ n-\text{odd}}} \left[a_n + b_n Z_{eq}(\pm\Delta f)\right] A^n \,, \tag{4}$$

Parameters a_n and b_n depend on carrier frequency, while Z_{eq} retains the dependence of IMD with modulation frequencies. Measurements can be fitted to the proposed model through a nonlinear least-squares optimization procedure provided that the set of measurements is wide enough. The

main difference with the case of the HEMT amplifier is the extraction of model parameters, which was done assuming a prior knowledge of the internal circuit structure, i.e. γ-functions in (3) were derived from the large-signal model of a HEMT transistor by using closed-form expressions. However, for a more complex commercial amplifier, there is no such knowledge about a_n and b_n.

III. Experimental results

A. Experimental setup

For the extraction of the model parameters or frequency response of the impedance, it is required a measurement setup that allows IM3 characterization in magnitude and phase, together with a power sweep. This characterization is carried out by using the method presented in [3]. The measurement setup, based on non-sophisticated communications equipment, is shown in Fig. 2. It is basically composed by a PC connected to the equipment with a general-purpose interface bus (GPIB), a Rohde & Schwarz SMIQ02B signal generator with the capability of modulating arbitrary waveforms, and an Agilent E4407B spectrum analyzer equipped with modulation analysis. The two tones are formed with a double-sideband suppressed-carrier signal modulated by a sinusoidal baseband waveform with frequency f_m, producing two coherent tones with the same level and an exactly constant separation $\Delta f = 2f_m$, which can be directly controlled. A restriction of the method is the existence of responses generated by the digital processing of the signal. However, these responses are more than 65 dB below the tones and allow margin enough to measure IM in practical situations without appreciable error.

Standard spectrum analyzer power measurement facilities are used for IMD magnitude measurements. For phase characterization, baseband samples in the time domain are recovered after the demodulator of the spectrum analyzer at a maximum sampling rate of 10 Ms/sec. By Fourier transforming the discrete samples, the recovered spectrum exhibits the relevant information in magnitude and phase. Considering that IM3 responses are spaced $3\Delta f$, IM3 products can be theoretically recovered for tones separated in frequency up to 3.3 MHz. As long as the narrowband condition is satisfied, any frequency dependence introduced by the spectrum analyzer to the relative phase measurement can be neglected.

B. HEMT amplifier results

A simple amplifier was constructed with the HEMT EPB018A5-70 of Excelics Semiconductors Inc. (Sunnyvale CA, USA) and characterized under several conditions. Two different biasing voltages, $V_{GS} = -0.24$ V and $V_{GS} = -0.4$ V, being $V_{DS} = 2$ V, and different input power levels were applied using a commercial Bias-T. Results for some of these measurements are shown in Figs. 3 and 4, the first one for the magnitude of $\mathrm{IM_{3H}}$ and the second one for the phases of $\mathrm{IM_{3H}}$ and $\mathrm{IM_{3L}}$ together with their phase difference. We can observe that circuit-level simulations accomplished using the SN approach (depicted with dashed line) only fit measurements for tone separations over 30 or 100 kHz, while the observed variations for lower two-tone separations can not be explained by purely electrical memory effects with the load impedance given by the employed commercial Bias-T.

The methodology described in Section II was applied to the measurements of $\mathrm{IM_{3L}}$ to extract the values of the equivalent load impedance $\bar{Z}_L$, whose inclusion in simulation leads to a perfect agreement with measurements even for small tone separations, between 10 and 30 kHz, as it is depicted with dotted line in Figs. 3 and 4. Then, part of the intrinsic model of the HEMT, the bias network, and the termination impedance were de-embedded and the best results were obtained when the hypothetical impedance Z_h was modeled as a series impedance placed between the intrinsic model of the amplifier and the bias network, as it is shown in Fig. 1(b). Finally, several simple circuit topologies for Z_h were tested and the best results were obtained for a parallel RC circuit. The model shown in Fig. 1(c) was employed to achieve more precise results. For all the studied conditions with this HEMT amplifier, the same configuration of $\bar{Z}_L$ and the same topology of Z_h produced the best adjustment. For the examples shown in Figs. 3 and 4, the optimized parameters for the elements of Z_h were the following:

- $R_1 = 444.9\,\Omega$, $C_1 = 0.25$ μF, $R_2 = 541.8\,\Omega$, and $C_2 = 0.22$ nF, for $V_{GS} = -0.24$ V and $P_{in} = -7$ dBm.
- $R_1 = 267\,\Omega$, $C_1 = 0.26$ μF, $R_2 = 318.3\,\Omega$, and $C_2 = 0.31$ nF, for $V_{GS} = -0.24$ V and $P_{in} = -5$ dBm.
- $R_1 = 966\,K\Omega$, $C_1 = 0.23$ μF, $R_2 = 976.2\,K\Omega$, and $C_2 = 0.023$ pF, for $V_{GS} = -0.4$ V and $P_{in} = -5$ dBm.

A good correspondence with measurements can be observed for all frequency separations in

the simulations for the magnitude of $\mathrm{IM}_{3\mathrm{H}}$ including the adjusted model for Z_h, which are shown with solid line in Fig. 3 for a bias voltage of $V_{GS} = -0.24$ V. We can observe that, increasing the input power level from -7 dBm to -5 dBm, the measured IM3 power does not follow the typical 3 dB/dB slope for the linear behavior because the input level is very close to the 1 dB compression point. However, the use of the equivalent load impedance achieves an appropriate agreement even for a mild nonlinear behavior.

Fig. 4 shows the phases of $\mathrm{IM}_{3\mathrm{H}}$ and $\mathrm{IM}_{3\mathrm{L}}$ and their phase difference for: (a) a bias point of $V_{GS} = -0.24$ V and an input level of -7 dBm, and (b) a bias point of $V_{GS} = -0.4$ V and an input level of -5 dBm. It should be noticed that the variation with frequency produced by memory effects can be observed more clearly in phase than in magnitude. Furthermore, it is more relevant for the bias voltage $V_{GS} = -0.4$ V, which is nearer the pinch-off voltage and produces a stronger nonlinearity in the amplifier. Again, a good agreement with measurements is achieved using a simple topology, even when a different bias condition and a higher input level are applied, increasing the importance of memory effects.

The models for the equivalent load impedance $\bar{Z}_L$ and the hypothetical impedance Z_h for a biasing voltage of $V_{GS} = -0.24$ V and input power levels of -7 dBm and -5 dBm are shown in the Smith Charts of Fig. 5.

C. Commercial amplifier results

In order to demonstrate the suitability of the impedance-based model approach not only for a HEMT circuit, the commercial amplifier MAX2430, manufactured by MAXIM Integrated Products (Sunnyvale CA, USA), has been modeled with the approach explained in Section II-B. This is a silicon medium power amplifier, with 16-pin QSOP package, operating in the frequency range between 800 and 1000 MHz, delivering 100 mW of output power at 915 MHz and exhibiting a gain over 30 dB with 3 V dc voltage and 60 mA current supply. For 0.6 V dc voltage the circuit operates as a class C amplifier. Above 2 V, the output stage is biased in class AB.

Although the device under test is a wideband amplifier at 915 MHz, the experimental characterization showed an asymmetry in the IM products, a clear indication of the existence of nonlinear memory effects. Four values of the input power per tone ranging from -25 to -10 dBm, were applied using a bias voltage of 3.6 V, and a sweep of 15 tone separations per level, around

915 MHz was performed to provide a grid of 60 complex values.

First, measurements were fitted to a model with 4 coefficients representing third- and fifth-order terms in (4), plus the unknown impedance. Fig. 6 shows the extracted impedance values $Z_{eq}(\Delta f)$ that minimize the square error. Considering the resemblance of this curve in the Smith Chart with that of a parallel resonant circuit, the hypothetical impedance was approximated by the impedance of an equivalent RLC circuit, depicted in solid line in the same figure. The parameter values of the parallel resonator were $R = 14.5\ \Omega$, $L = 5.4\ \mu$H, and $C = 5.4\ \mu$F. The model with the resonant circuit and calculated coefficients $\{a_n, b_n\}$ was then tested to simulate IM3 products and asymmetries. Although it showed a very good correspondence for the highest measured power level, the agreement was not as good for low power levels, due to the high dynamic range of the IMD values used for the adjustment. Using 6 coefficients, the dynamic range of the model is increased accordingly, as Fig. 7 shows, which compares predicted and measured IM3 phase asymmetry in the full range of input levels and tone spacings. Magnitude levels of $\mathrm{IM_{3H}}$ for this model are also depicted in Fig. 8. Simulated $\mathrm{IM_{3L}}$ exhibits a similar correspondence with measurement data.

CONCLUSIONS

In this paper we have proposed a frequency domain model that predicts two-tone IM3 responses in amplifiers, in magnitude and phase, and their dependence with tone spacing. The impedance-based model is obtained by comparing input and output waveforms. Firstly, a HEMT circuit has been analyzed and the use of a hypothetical load impedance has been justified to capture memory effects of thermal origin. Then an extension for more complex commercial amplifiers has been presented, for which no knowledge about the internal structure of the circuit is required. The close correspondence between the measured and modeled data demonstrates the ability of this approach to capture memory effects using a simple model parameter extraction, even when the amplifier is driven near saturation, which corresponds to a common situation in the real practice, for which the impact of memory effects is critical and requires a careful modeling.

The equivalent hypothetical impedance gives the model a structural significance, since it identifies a circuit element playing a major role in the generation of memory effects, regardless they are of electrical or thermal origin. Circuit designers can gain some insight from this

impedance to devise efficient linearizers. We can remark that, in the case of the HEMT device, the modeled circuit is a low-pass filter placed between the drain and source nodes. The proposed Z_h, although electrical, plays an analogous role to that of a thermal impedance [8]. As it is stated in [2], the thermal impedance in the active device is not purely resistive, but forms a distributed low-pass filter, which means that the temperature changes caused by the dissipated power are frequency-dependent and cause thermal memory effects.

Further work is needed to extend the model to other modulation formats, although the impedance impulse response seems a promising approach to develop an equivalent signal-independent behavioral model in the time domain. This approach can make possible some contributions to the large-signal modeling of devices, including thermal memory effects that affect low modulation frequencies.

ACKNOWLEDGMENTS

This work has been partially funded by the Spanish Board of Scientific and Technological Research (CICYT) under grant TEC2004-06451-C05-03/TCM.

REFERENCES

[1] W. Bosch and G. Gatti, Measurement and simulation of memory effects in predistortion linearizers, IEEE Transactions on Microwave Theory and Techniques 37 (12), pp. 1885–1890, Dec. 1989.

[2] J. K. Vuolevi, T. Rahkonen, and J. P. Manninen, Measurement Technique for Characterizing Memory Effects in RF Power Amplifiers, IEEE Transactions on Microwave Theory and Techniques, 49 (8), pp. 1383–1389, Aug. 2001.

[3] C. Crespo-Cadenas, J. Reina-Tosina, and M. J. Madero-Ayora, Phase characterization of two-tone intermodulation distortion, 2005 IEEE MTT-S Int. Microwave Symp. Dig., pp. 1505–1508, Jun. 2005.

[4] C. Crespo-Cadenas, J. Reina-Tosina, and M. J. Madero-Ayora, IM3 and IM5 phase characterization and analysis based on a simplified Newton approach, IEEE Transactions on Microwave Theory and Techniques, pp. 321–328, Jan. 2006.

[5] M. J. Madero-Ayora, J. Reina-Tosina, and C. Crespo-Cadenas, Phase characterization of intermodulation products including electrothermal memory effects, Proc. Integrated Nonlinear Microwave and Millimetre-wave Circuits, pp. 56–59, Jan. 2006.

[6] J. Reina-Tosina, M. J. Madero-Ayora, and C. Crespo-Cadenas, An Impedance-based Model for the Evaluation of IM3 in Commercial Amplifiers with Memory, 2006 IEEE Wireless and Microwave Technology Conference Proc., 4 pages, Dec. 2006.

[7] J. Brinkhoff and A. E. Parker, Effect of Baseband Impedance on FET Intermodulation, IEEE Transactions on Microwave Theory and Techniques, 51 (3), pp. 1045–1051, Mar. 2003.

[8] S. Boumaiza and F. M. Ghannouchi, Thermal memory effects modeling and compensation in RF power amplifiers and predistortion linearizers, IEEE Transactions on Microwave Theory and Techniques, 51 (12), pp. 2427–2433, Dec. 2003.

List of Figures

1 Equivalent circuit of a HEMT amplifier, including the proposed model for the equivalent load impedance. 13
2 Equipment setup for two-tone IMD characterization. 13
3 Measured magnitude of upper IM3 products for a HEMT amplifier at input levels of -7 and -5 dBm per tone and a bias voltage $V_{gs} = -0.24$ V, including predictions. 14
4 Measured phase and phase difference of IM3 products for a HEMT amplifier at different input levels and bias voltages, including predictions. 15
5 Smith Chart with the extracted values of the equivalent hypothetical load impedance and its RC circuit model for a HEMT amplifier with a bias voltage $V_{gs} = -0.24$ V. 16
6 Zoom in the Smith Chart with the extracted values of the equivalent load impedance and its RLC circuit model for a commercial amplifier. 17
7 Measured two-tone phase asymmetries and prediction for a commercial amplifier. . 18
8 Measured magnitude of upper IM3 products and prediction for a commercial amplifier. 19

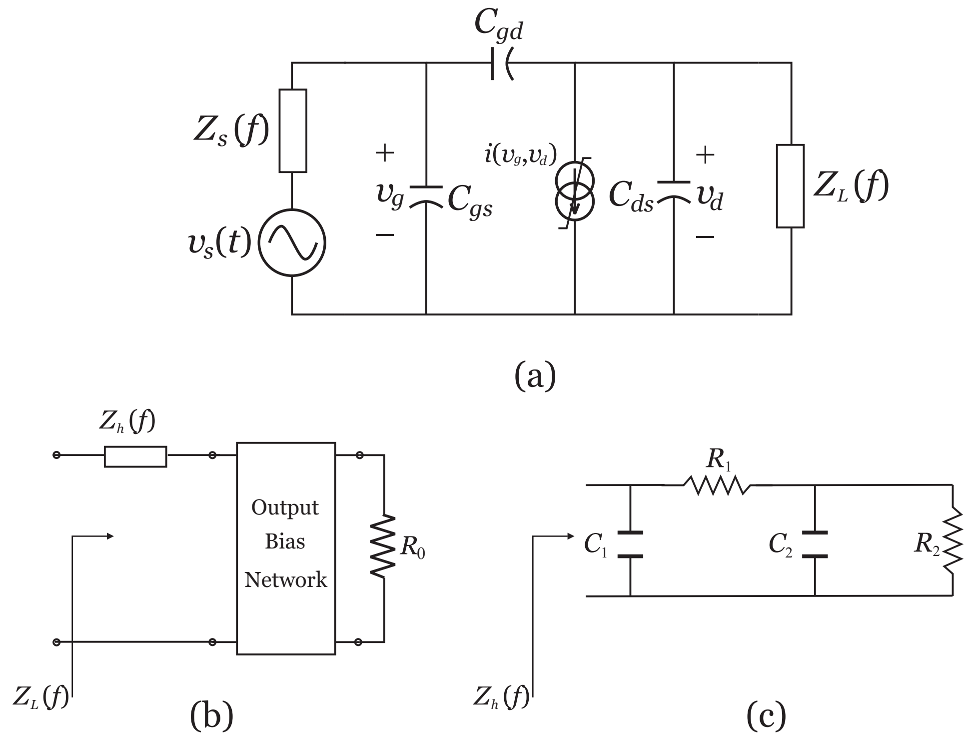

Fig. 1. Equivalent circuit of a HEMT amplifier used in the analysis (a). Proposed model for the equivalent load impedance $\bar{Z}_L$ (b) and the hypothetical impedance Z_h (c).

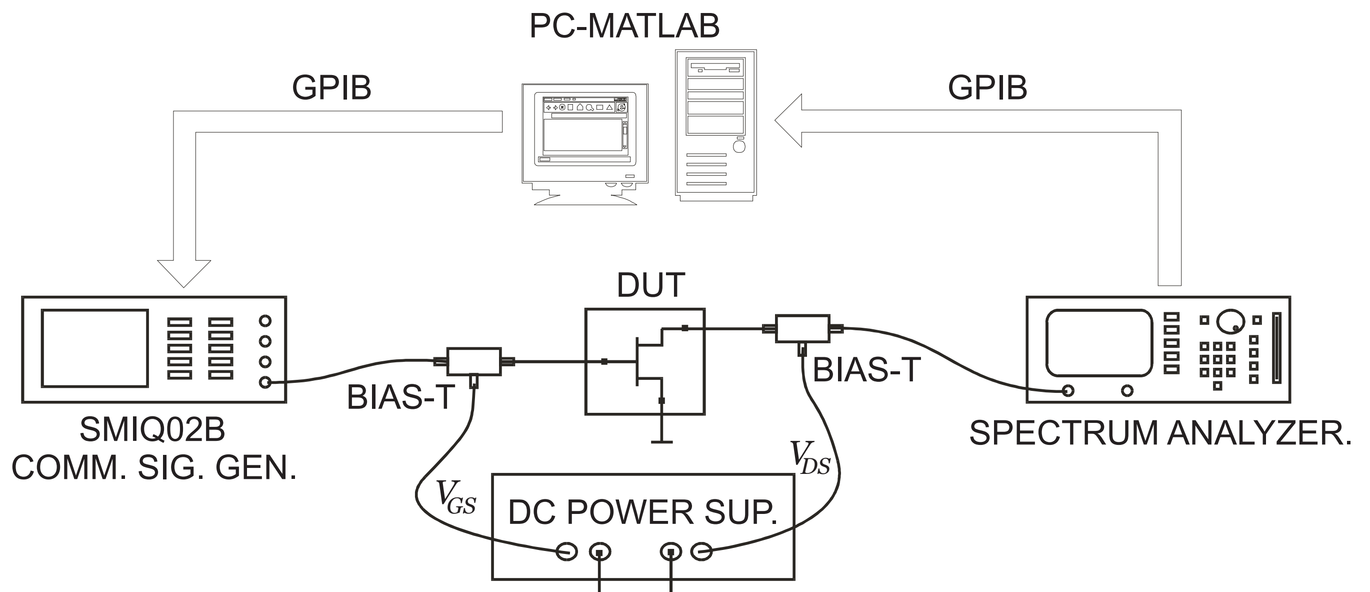

Fig. 2. Equipment setup for two-tone IMD characterization.

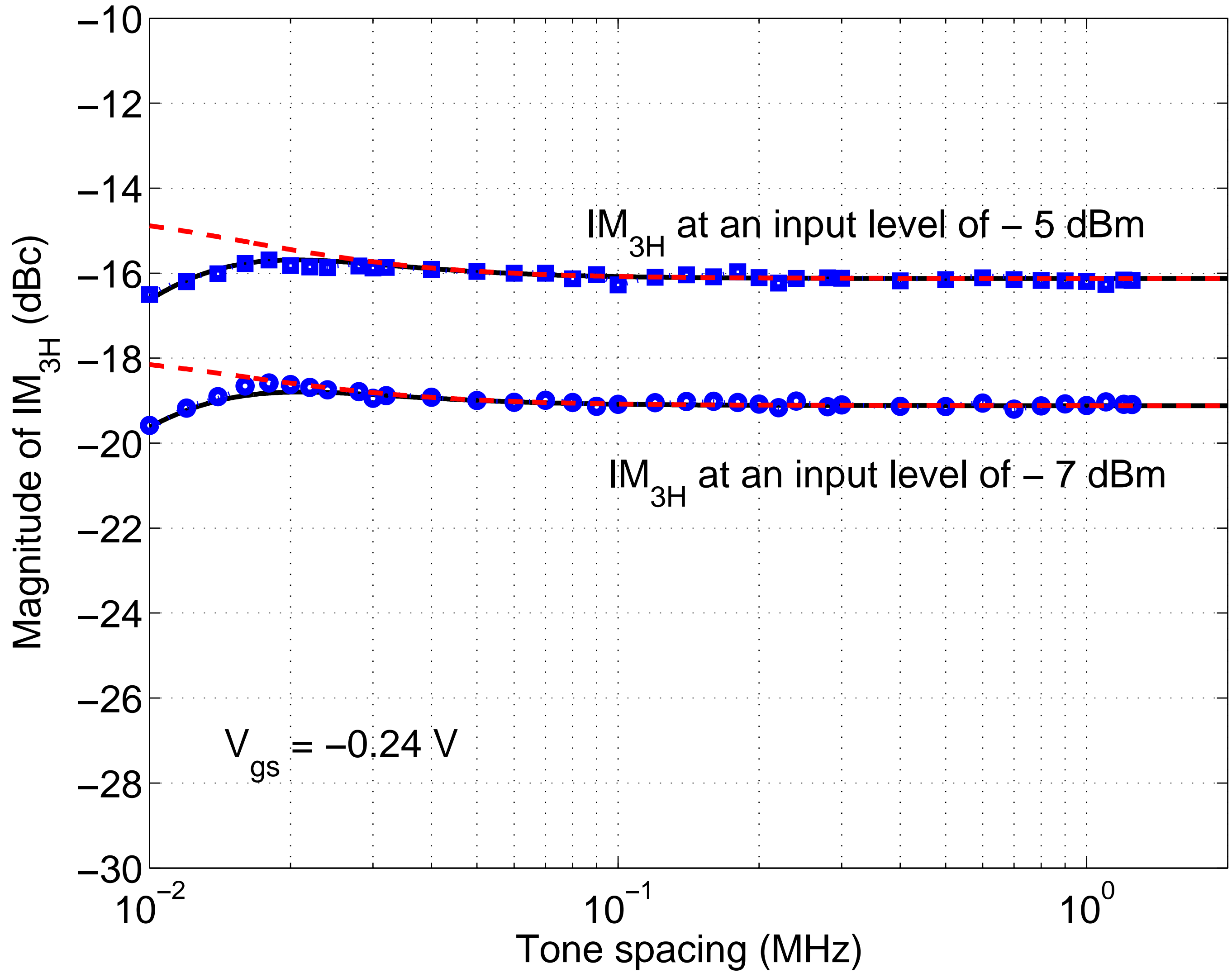

Fig. 3. Measured magnitude of upper IM3 products for a HEMT amplifier at input levels of -7 dBm (circles) and -5 dBm (squares) per tone and a bias voltage $V_{gs} = -0.24$ V. Predictions without the hypothetical load impedance (dashed line), with the extracted values of the hypothetical load impedance (dotted line) and with the chosen circuit model (solid line).

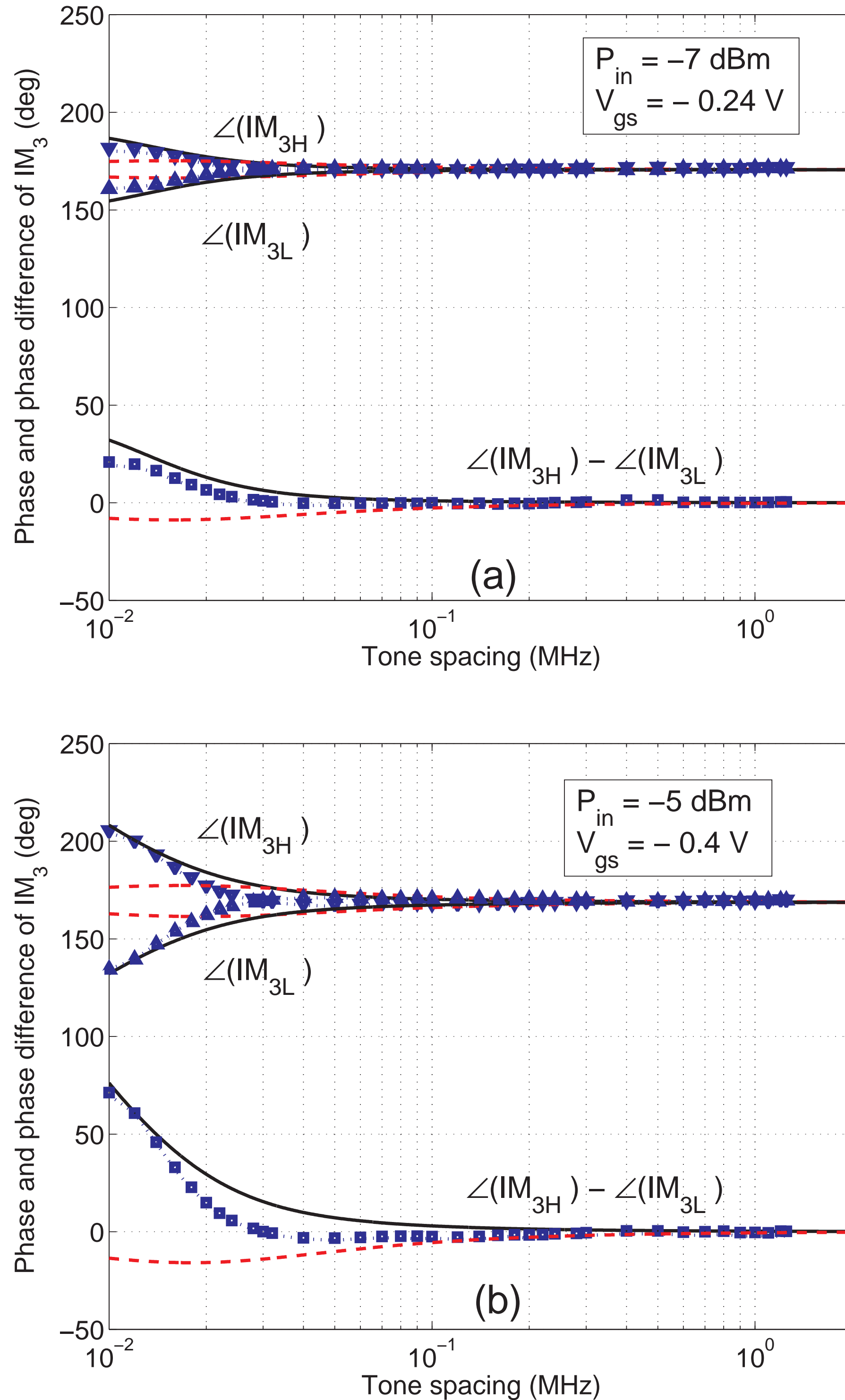

Fig. 4. Measured phase (triangles) of upper and lower IM3 products and phase difference (squares) for a HEMT amplifier with $P_{in} = -7$ dBm per tone and $V_{gs} = -0.24$ V (a) and $P_{in} = -5$ dBm per tone and $V_{gs} = -0.4$ V (b). Predictions without the hypothetical load impedance (dashed line), with the extracted values of the hypothetical load impedance (dotted line) and with the chosen circuit model (solid line).

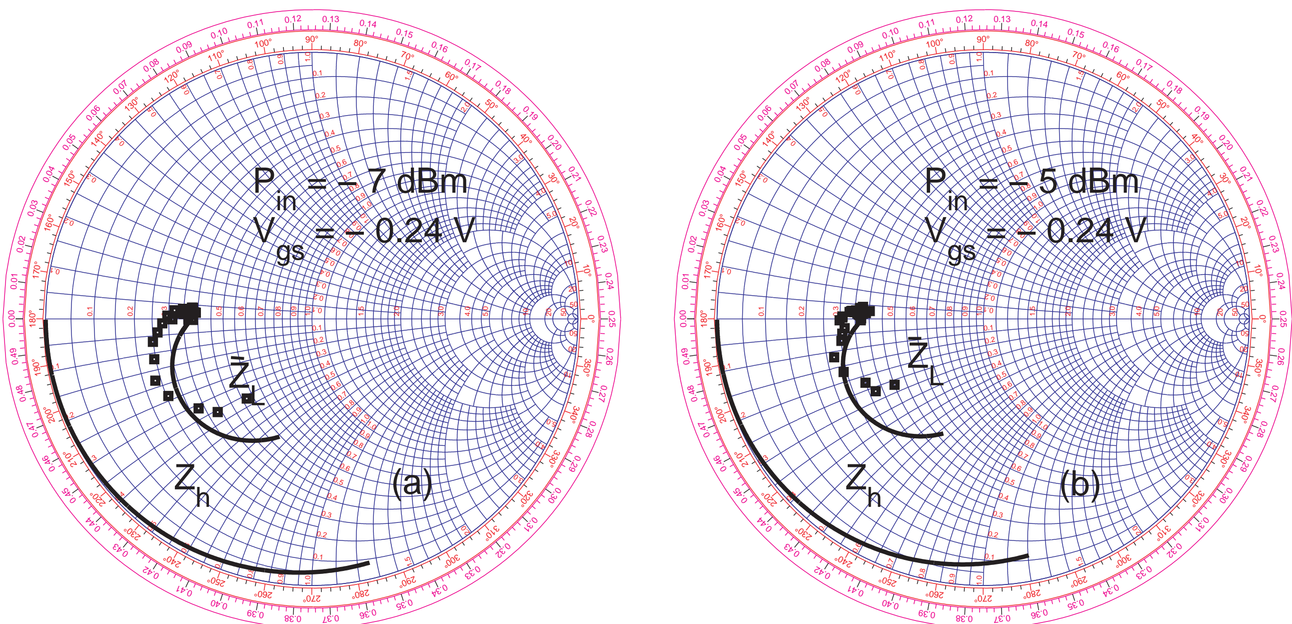

Fig. 5. Smith Chart with the extracted values of the equivalent hypothetical load impedance at baseband frequencies (marks) for a HEMT amplifier at input levels of -7 dBm (a) and -5 dBm (a) for a bias voltage $V_{gs} = -0.24$ V. The solid lines represent the impedance of a parallel resonant RC circuit that best approximates the extracted values in least-squares sense (Z_h) and the equivalent load impedance including this RC circuit ($\bar{Z}_L$).

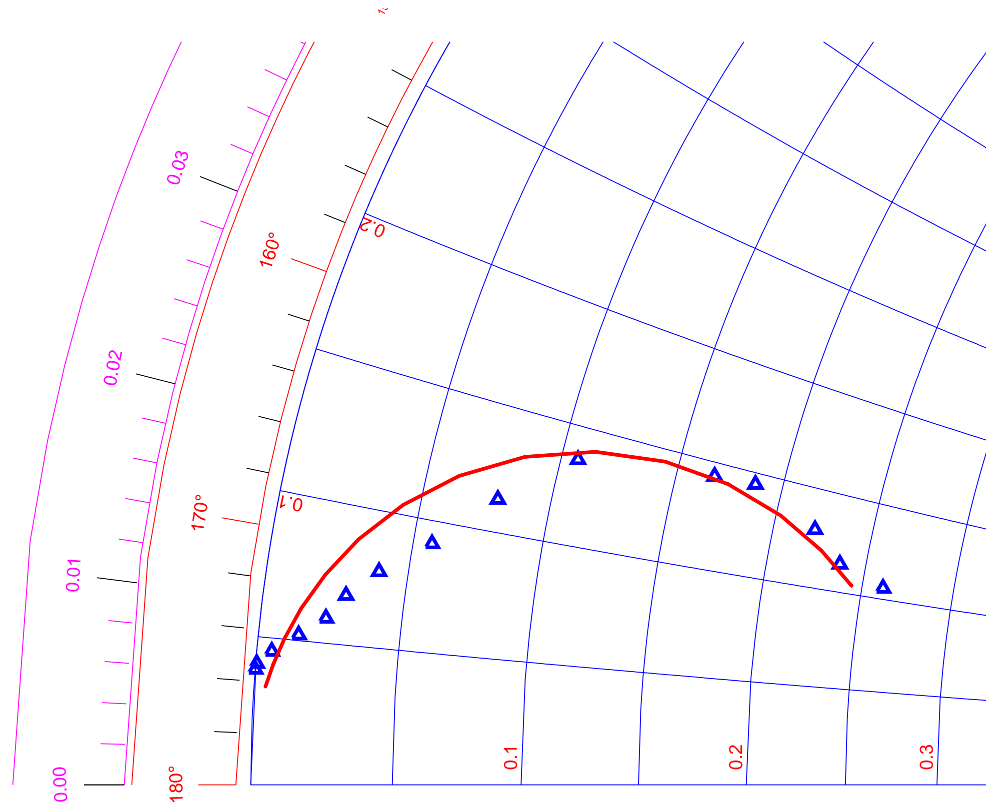

Fig. 6. Zoom in the Smith Chart with the extracted values of the equivalent load impedance at baseband frequencies (marks) for a commercial amplifier. The solid line represents the impedance of a parallel resonant RLC circuit that best approximates the extracted values in least-squares sense.

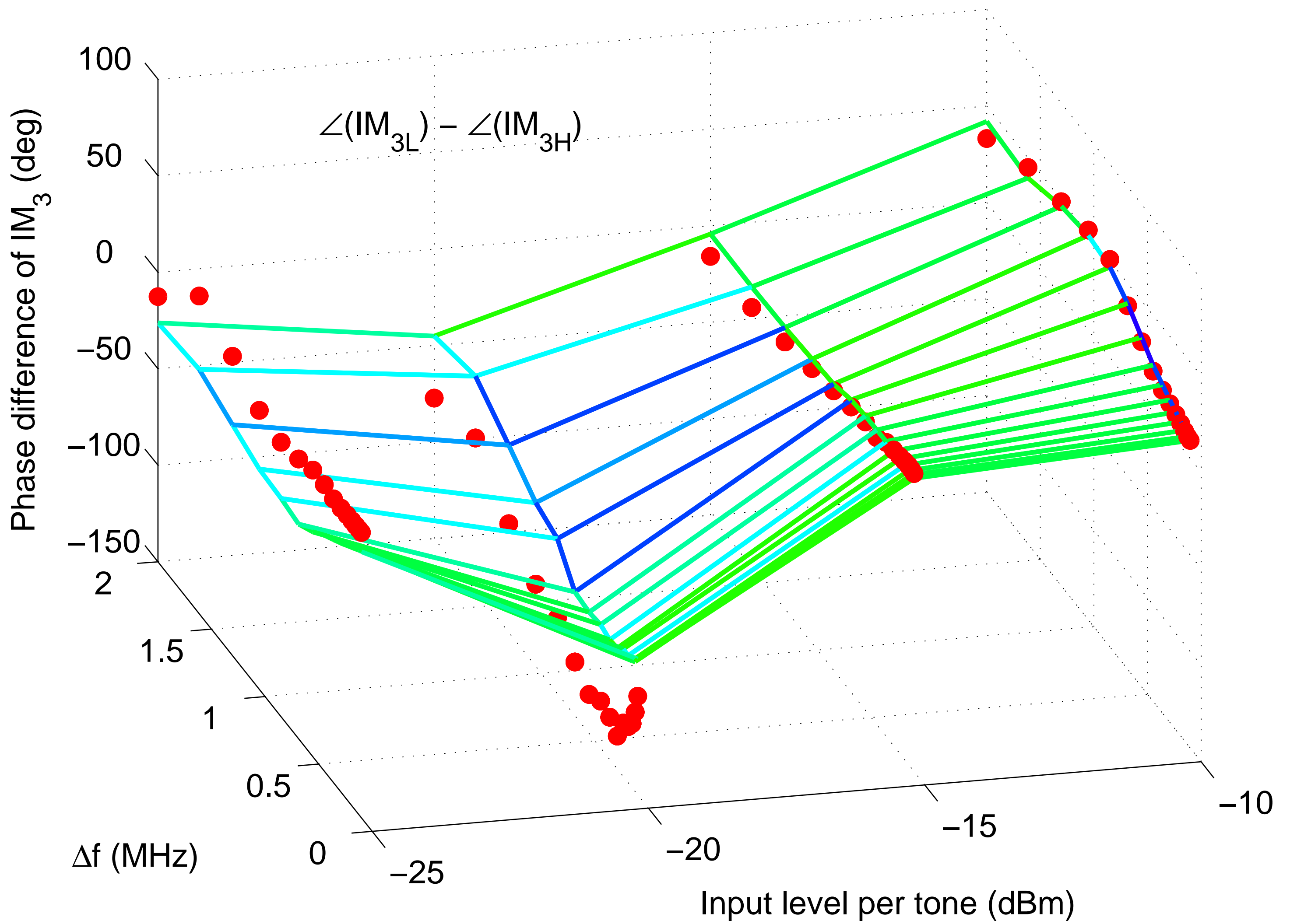

Fig. 7. Measured two-tone IM3 phase asymmetries between lower and upper products (marks) and prediction (wireframe) with the extracted values of the equivalent load impedance using a model with 6 parameters for a commercial amplifier.

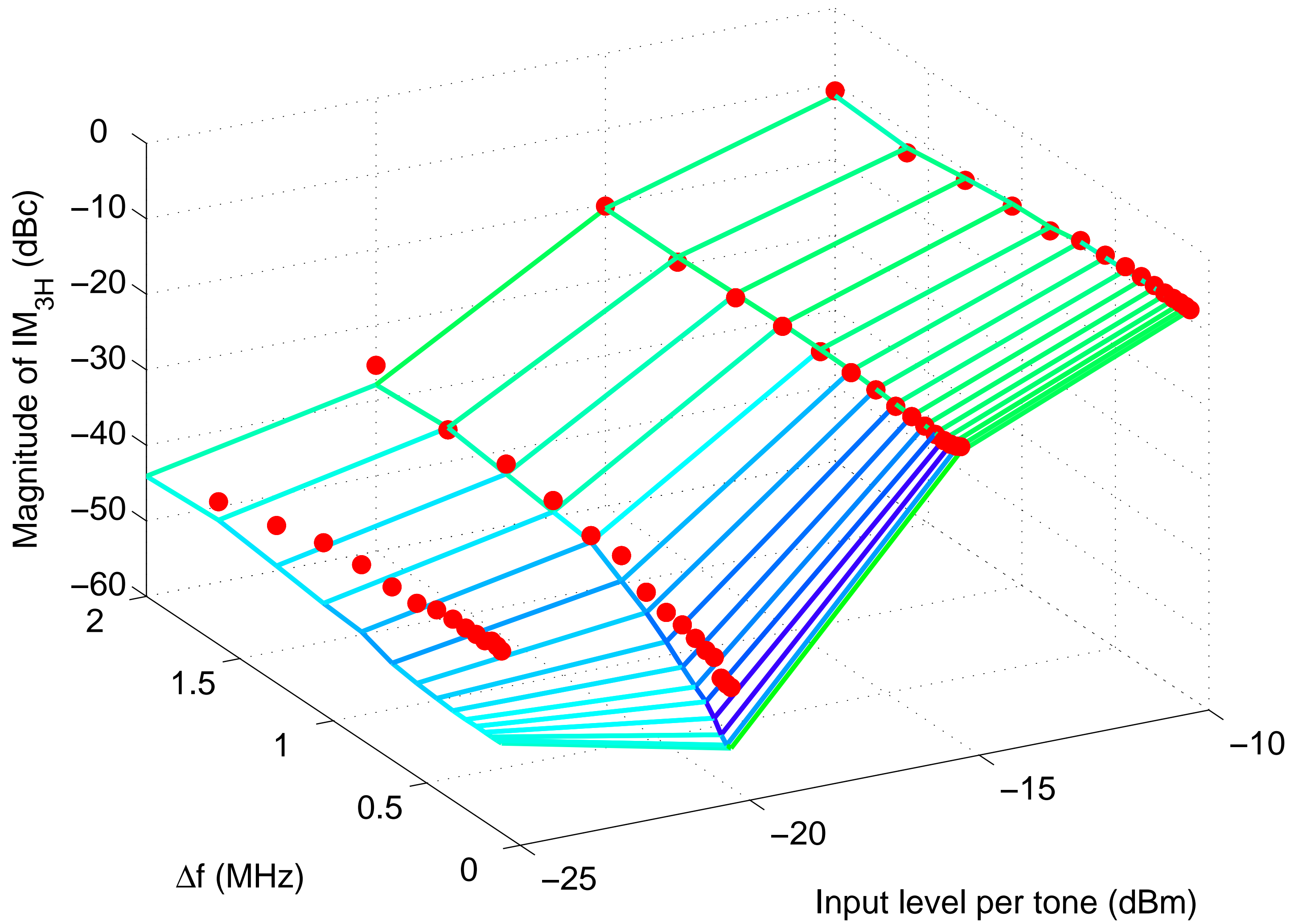

Fig. 8. Measured magnitude of upper IM3 products (marks) and prediction (wireframe) with the extracted values of the equivalent load impedance using a model with 6 parameters for a commercial amplifier.